

# Consumable Double-Electrode GMAW Part II: Monitoring, Modeling, and Control

*Selecting bypass arc voltage, proposing an interval control algorithm, and conducting step responses along with closed-loop control experiments for this process were undertaken*

BY K. H. LI AND Y. M. ZHANG

**ABSTRACT.** Consumable double-electrode gas metal arc welding (DE-GMAW) is an innovative welding process that can significantly increase the deposition rate without raising the base metal heat input to an undesired level. To be qualified as a practical manufacturing process, feedback control is required to ensure the presence and stability of the bypass arc. To this end, the bypass arc voltage was selected to monitor the state of the bypass arc. Further, the authors proposed an interval control algorithm for models whose parameters are bounded by given intervals. This algorithm does not require the specific values for parameters, but only their intervals, which can be identified through a selected set of experiments. By conducting step responses under different conditions, a few models were obtained and the parameter intervals were determined and enlarged to increase the stability margin. Using the obtained parameter intervals in the interval control algorithm, closed-loop control experiments have been conducted to verify the effectiveness of the proposed control system for the consumable DE-GMAW process.

## Introduction

The consumable DE-GMAW was implemented by adding another gas metal arc welding (GMAW) gun and constant current (CC) power supply to a conventional GMAW setup — Fig. 1. The CC power supply provides the bypass current and the constant voltage (CV) power supply provides the base metal current. The total melting current, which melts the main welding wire, thus is the sum of the bypass current and base metal current:  $I = I_1 + I_2$ . (Here the base metal current is denoted as  $I_1$  or  $I_{bm}$  and the bypass current is denoted as  $I_2$  or  $I_{bp}$ . This notation also applies to other variables or parameters, such as arc voltage and

wire feed speed:  $V_1, V_2, WFS_1$ , and  $WFS_2$ .) The bypass welding wire is primarily melted by the bypass current, and the base metal is primarily heated by the base metal current. Hence, it is possible to use a high total melting current for increased deposition rate, while maintaining a low base metal current and heat input. An additional deposition rate increase is obtained from the bypass wire, which is primarily melted by the bypass current.

However, as discussed in Part I, without proper control the process can only remain stable when the welding parameters are carefully selected and do not vary in large ranges. If the process becomes unstable and the bypass arc extinguishes periodically, the bypass loop would break and all the melting current would be imposed onto the base metal. Such a large base metal current can melt through and damage the workpiece. Thus, to ensure the consumable DE-GMAW process functions properly, its stability must be controlled and guaranteed. To this end, an appropriate signal must be found to characterize the process stability. This signal must accurately reflect the process stability and be monitored conveniently in a manufacturing environment. Then a process model can be obtained to design a suitable control algorithm. Hence, this paper (Part II) is devoted to the monitoring, modeling, and control of the consumable DE-GMAW process.

## Stability Monitoring

### Vision Signal

The most direct indication of stability is obtained by monitoring the bypass arc,

especially the location of the tip of the bypass welding wire in relation to the main arc. Experiments show that when the bypass arc is stable, the tip of the bypass welding wire must be close enough to the main arc. However, machine vision (Ref. 1) requires an imaging system, which should be installed to and move with the welding torch. This makes the welding system complicated. Machine vision may not be the most preferable method for welding processes.

### Sound Signal

Usually there is a characteristic sound in welding associated with each particular operating mode. For example, in plasma arc welding there is a characteristic sound when the keyhole is established. In GMAW, the sound can vary quite drastically and is dependent on the mode of metal transfer. A similar phenomenon was observed in the consumable DE-GMAW. For instance, when the bypass arc was unstable, the sound was hard and accompanied by spatters. But once the bypass arc became stable, the metal transfer became a spray transfer mode because of the high melting current, thus there was no spatters and sharp sound.

### Thermal Signal

Thermal signal reflects the temperature field, which heavily depends on the distance for a specific thermal point. Take the consumable DE-GMAW process as an example: the bypass arc can be seen as a thermal point. In the axis direction of the bypass welding wire, different positions will have different temperatures depending on their distances from the welding arc. Thus, a fixed position thermal coupler theoretically can be used to monitor the relative movement of the tip of the bypass welding wire.

### Current Signal

Current signal is often used in welding processes. It has been successfully used in

## KEYWORDS

Double Electrode  
Arc Welding  
Melting Rate  
Interval Model  
Welding Controls  
Heat Input

K. H. LI (Kehai.Li@esab.com) is a PhD student and Y. M. ZHANG (ymzhang@enr.uky.edu) is a Professor of Electrical Engineering with the Center for Manufacturing and Department of Electrical and Computer Engineering, University of Kentucky, Lexington, Ky.

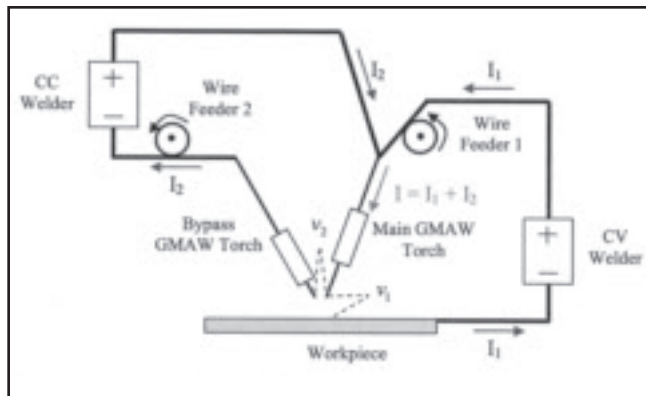


Fig. 1 — Consumable DE-GMAW system.

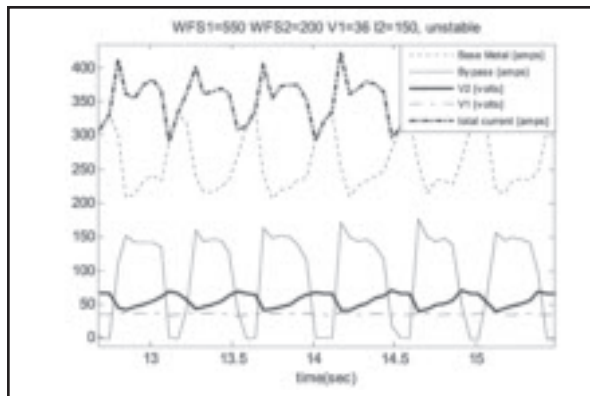


Fig. 2 — Behavior of an unstable bypass arc.

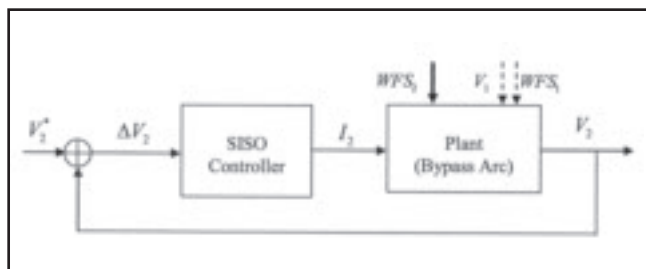


Fig. 3 — Proposed closed-loop system.

Table 1 — Impulse Intervals

$j$	$0.8 h_{\min}(j)$ (V/A)	$1.2 h_{\max}(j)$ (V/A)
1	0.0099	0.0190
2	0.0070	0.0122
3	0.0047	0.0080
4	0.0030	0.0055
5	0.0019	0.0038
6	0.0012	0.0027
7	0.0008	0.0019
8	0.0005	0.0014
9	0.0003	0.0010
10	0.0002	0.0007
11	0.0001	0.0005
12	0.0001	0.0004
13	0.0001	0.0003
14	0	0.0002
15	0	0.0001
16	0	0.0001

double-sided arc welding (DSAW) to detect the establishment of the keyhole (Refs. 2, 3). In DE-GMAW, the bypass current can tell the existence of the bypass arc. However, because the bypass power supply is a CC welding machine, the bypass current does not change with the arc length. Figure 2 illustrates an experiment with the following parameters:  $WFS_1 = 14$  m/min (550 in./min),  $V_1 = 36$  V,  $WFS_2 = 5.1$  m/min (200 in./min), and  $I_2 = 150$  A. The bypass current was set to a high value to make the bypass arc unstable. It can be

seen that the bypass current was present once the bypass arc was ignited. When the bypass arc became longer and longer, the bypass current did not change. Once the bypass arc extinguished, the bypass current dropped to zero abruptly. Thus, the bypass current can only indicate two discrete states: bypass arc on or bypass arc off, but not the trend to become unstable.

### Voltage Signal

Arc voltage signals — arc length (Refs. 4, 5), for example — are often used to monitor welding processes. Normally, the arc voltage is proportional to the arc length. The following can be observed during DE-GMAW experiments:

1. The bypass arc voltage is equal to the main arc voltage when the bypass welding wire touches the workpiece. This happens when the bypass wire feed speed is too fast.
2. When the length of the bypass arc increases,  $V_2$  increases as illustrated in Fig. 2.
3. There is an optimal  $V_2$  that appears to establish an optimal operating point to

stabilize the process.

4. When the bypass arc tends to extinguish,  $V_2$  tends to increase to a high level. The arc voltage can thus reflect the state of the bypass arc. The state of the bypass arc can be predicted from the bypass arc voltage. Hence, the bypass arc voltage may be used to characterize the stability of the consumable DE-GMAW process.

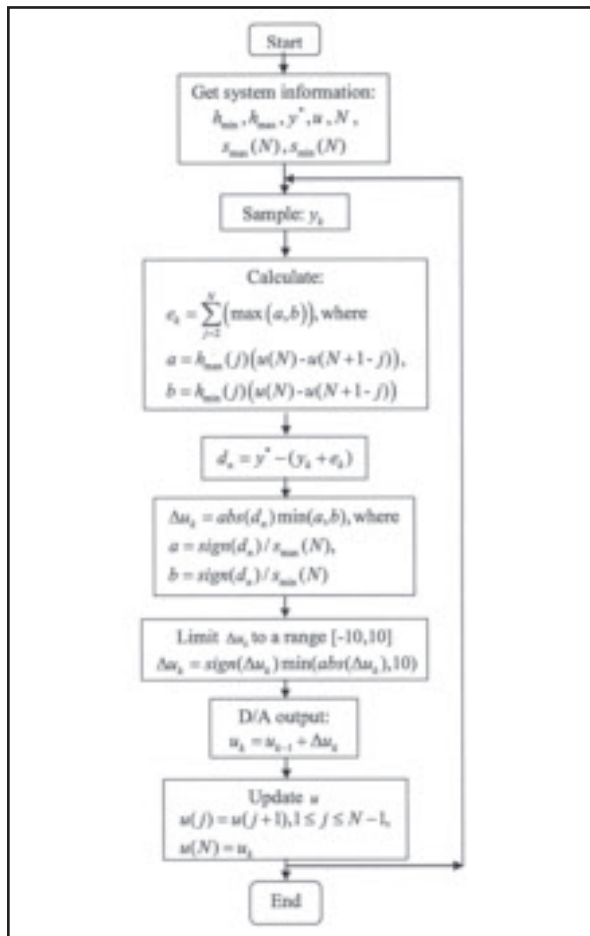


Fig. 4 — Flowchart of the control algorithm.

# Consumable Double-Electrode GMAW Part II: Monitoring, Modeling, and Control

*Selecting bypass arc voltage, proposing an interval control algorithm, and conducting step responses along with closed-loop control experiments for this process were undertaken*

BY K. H. LI AND Y. M. ZHANG

**ABSTRACT.** Consumable double-electrode gas metal arc welding (DE-GMAW) is an innovative welding process that can significantly increase the deposition rate without raising the base metal heat input to an undesired level. To be qualified as a practical manufacturing process, feedback control is required to ensure the presence and stability of the bypass arc. To this end, the bypass arc voltage was selected to monitor the state of the bypass arc. Further, the authors proposed an interval control algorithm for models whose parameters are bounded by given intervals. This algorithm does not require the specific values for parameters, but only their intervals, which can be identified through a selected set of experiments. By conducting step responses under different conditions, a few models were obtained and the parameter intervals were determined and enlarged to increase the stability margin. Using the obtained parameter intervals in the interval control algorithm, closed-loop control experiments have been conducted to verify the effectiveness of the proposed control system for the consumable DE-GMAW process.

## Introduction

The consumable DE-GMAW was implemented by adding another gas metal arc welding (GMAW) gun and constant current (CC) power supply to a conventional GMAW setup — Fig. 1. The CC power supply provides the bypass current and the constant voltage (CV) power supply provides the base metal current. The total melting current, which melts the main welding wire, thus is the sum of the bypass current and base metal current:  $I = I_1 + I_2$ . (Here the base metal current is denoted as  $I_1$  or  $I_{bm}$  and the bypass current is denoted as  $I_2$  or  $I_{bp}$ . This notation also applies to other variables or parameters, such as arc voltage and

wire feed speed:  $V_1, V_2, WFS_1$ , and  $WFS_2$ .) The bypass welding wire is primarily melted by the bypass current, and the base metal is primarily heated by the base metal current. Hence, it is possible to use a high total melting current for increased deposition rate, while maintaining a low base metal current and heat input. An additional deposition rate increase is obtained from the bypass wire, which is primarily melted by the bypass current.

However, as discussed in Part I, without proper control the process can only remain stable when the welding parameters are carefully selected and do not vary in large ranges. If the process becomes unstable and the bypass arc extinguishes periodically, the bypass loop would break and all the melting current would be imposed onto the base metal. Such a large base metal current can melt through and damage the workpiece. Thus, to ensure the consumable DE-GMAW process functions properly, its stability must be controlled and guaranteed. To this end, an appropriate signal must be found to characterize the process stability. This signal must accurately reflect the process stability and be monitored conveniently in a manufacturing environment. Then a process model can be obtained to design a suitable control algorithm. Hence, this paper (Part II) is devoted to the monitoring, modeling, and control of the consumable DE-GMAW process.

## Stability Monitoring

### Vision Signal

The most direct indication of stability is obtained by monitoring the bypass arc,

especially the location of the tip of the bypass welding wire in relation to the main arc. Experiments show that when the bypass arc is stable, the tip of the bypass welding wire must be close enough to the main arc. However, machine vision (Ref. 1) requires an imaging system, which should be installed to and move with the welding torch. This makes the welding system complicated. Machine vision may not be the most preferable method for welding processes.

### Sound Signal

Usually there is a characteristic sound in welding associated with each particular operating mode. For example, in plasma arc welding there is a characteristic sound when the keyhole is established. In GMAW, the sound can vary quite drastically and is dependent on the mode of metal transfer. A similar phenomenon was observed in the consumable DE-GMAW. For instance, when the bypass arc was unstable, the sound was hard and accompanied by spatters. But once the bypass arc became stable, the metal transfer became a spray transfer mode because of the high melting current, thus there was no spatters and sharp sound.

### Thermal Signal

Thermal signal reflects the temperature field, which heavily depends on the distance for a specific thermal point. Take the consumable DE-GMAW process as an example: the bypass arc can be seen as a thermal point. In the axis direction of the bypass welding wire, different positions will have different temperatures depending on their distances from the welding arc. Thus, a fixed position thermal coupler theoretically can be used to monitor the relative movement of the tip of the bypass welding wire.

### Current Signal

Current signal is often used in welding processes. It has been successfully used in

## KEYWORDS

Double Electrode  
Arc Welding  
Melting Rate  
Interval Model  
Welding Controls  
Heat Input

K. H. LI (Kehai.Li@esab.com) is a PhD student and Y. M. ZHANG (ymzhang@enr.uky.edu) is a Professor of Electrical Engineering with the Center for Manufacturing and Department of Electrical and Computer Engineering, University of Kentucky, Lexington, Ky.

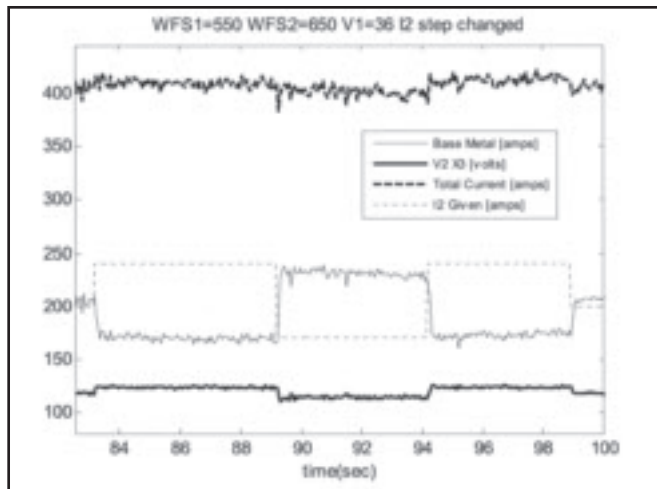


Fig. 5 — Step response experiment with  $WFS_2 = 650$  in./min.

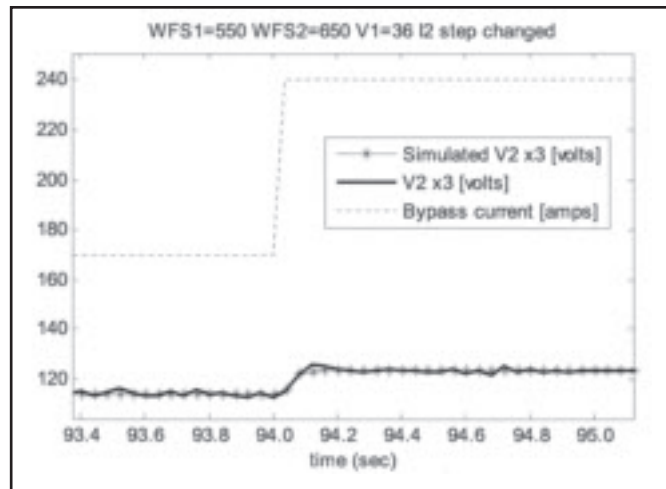


Fig. 6 — Step response when bypass current increased from 170 to 240 A with  $WFS_2 = 650$  in./min.

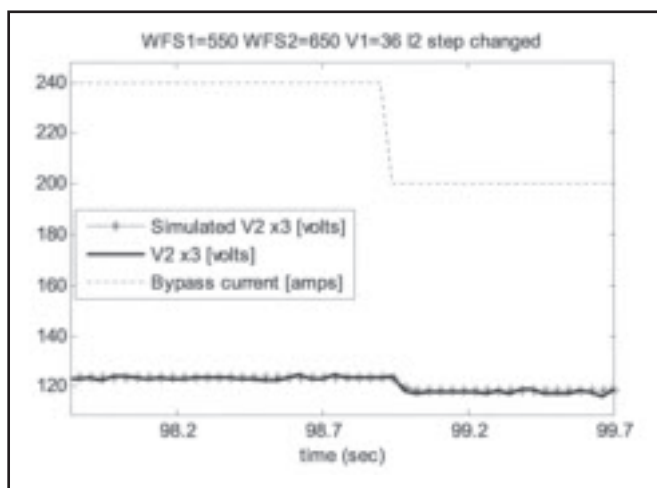


Fig. 7 — Step response when bypass current decreased from 240 to 200 A with  $WFS_2 = 650$  in./min.

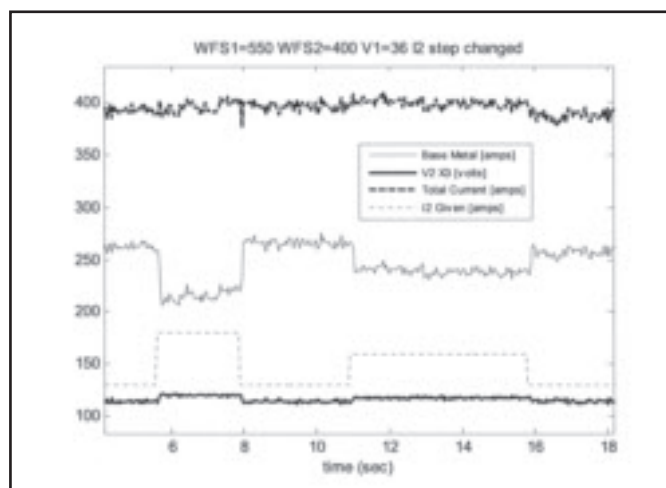


Fig. 8 — Step response experiment with  $WFS_2 = 400$  in./min.

## Process Analysis

As discussed earlier, the consumable DE-GMAW process has two parallel arcs: the main arc established between the main welding wire and the workpiece, and the bypass arc established between the main welding wire and the bypass welding wire. The main welding wire is the common anode of the two arcs, and its melting is determined by the sum of the two currents or the total current.

When the main wire feed speed ( $WFS_1$ ) and arc voltage ( $V_1$ ) are given, the total current is approximately fixed. The use of the CV power supply ensures a constant distance from the tip of the main welding wire to the workpiece (between them  $V_1$  is measured). This distance is not affected by variations in the bypass arc length.

The bypass welding wire is primarily melted by the cathode heat of the bypass arc. The bypass current ( $I_2$ ) needed for a

given bypass wire feed speed is approximately fixed, even though a perturbation is introduced for  $WFS_2$ . In fact, if  $WFS_2$  is increased, the cathode heat would become insufficient to melt the bypass welding wire. As a result, the distance from the contact tube to the tip of the bypass welding wire will increase, and the extension of the bypass welding wire increases. In the meantime, the resistive heat (proportional to  $I_2^2$  and the stickout length (Refs. 6, 7)) also increases. If  $WFS_2$  is decreased, the cathode heat will tend to melt the bypass welding wire faster, but a reduced extension will reduce the resistive heat. In both cases, new equilibriums will be reestablished at different locations, but the measured  $V_2$  will be changed. The process shifts from the optimal condition. To maintain the stability, the authors proposed to adjust the cathode heat to maintain the bypass welding wire at its optimal location in relation to the main welding wire.

The previous discussion and analysis suggest that the process to be controlled for the bypass arc stability can be defined as a dynamic system with  $V_2$  as the output and  $I_2$  as the input. It appears that the dynamic model, which correlates the input and output, may be affected by the bypass wire feed speed, but possible effects from  $WFS_1$  and  $V_1$  setting should not be significant. This implies that the dynamic model established using a particular  $WFS_2$  may be just a local model. When a different  $WFS_2$  is used, the process dynamics may be subject to change.

As can be seen, the control of the bypass arc stability requires the bypass current be adjusted in real time. Although the base metal current will change with the bypass current, the stability of the main arc will be maintained by the CV power supply. When  $WFS_2$  and the desired  $V_2$  setting are given, the required  $I_2$  is approximately fixed and the real-time adjustment of  $I_2$

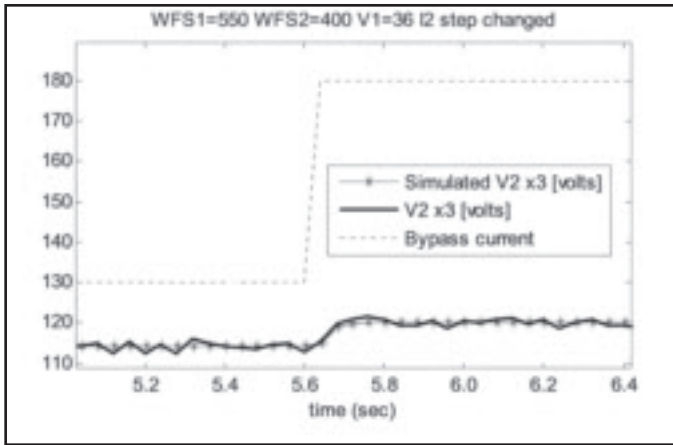


Fig. 9 — Step response when bypass current increased from 130 to 180 A with  $WFS_2 = 400$  in./min.

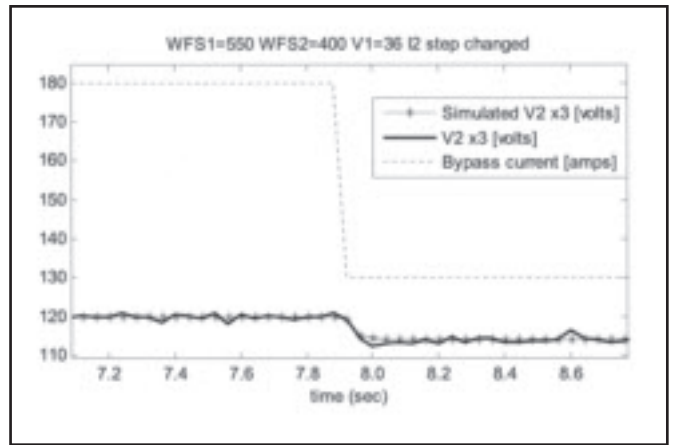


Fig. 10 — Step response when bypass current decreased from 180 to 130 A with  $WFS_2 = 400$  in./min.

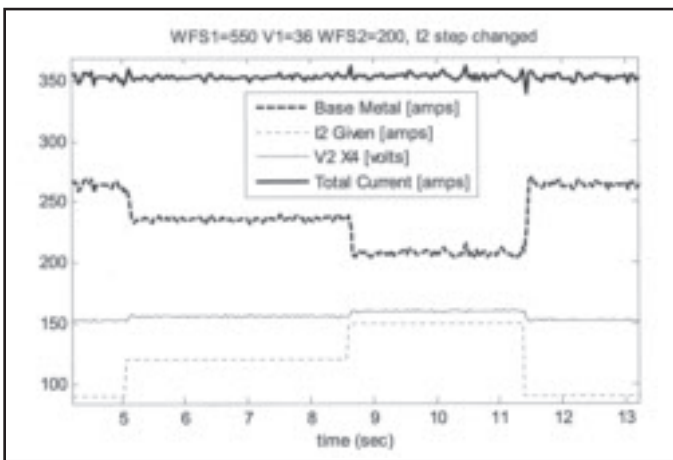


Fig. 11 — Step response experiment with  $WFS_2 = 200$  in./min.

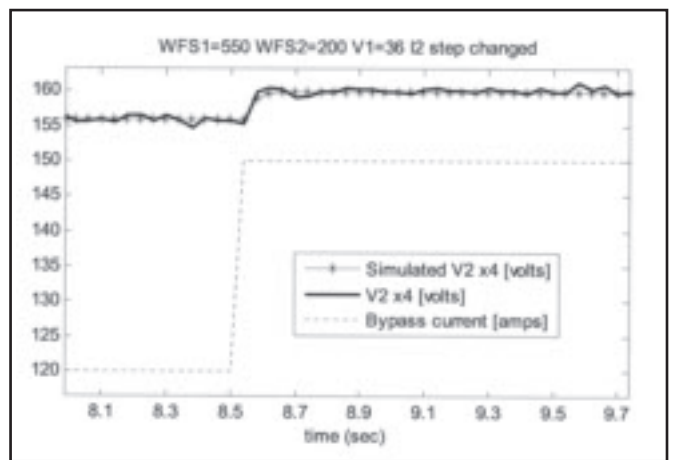


Fig. 12 — Step response when bypass current increased from 120 to 150 A with  $WFS_2 = 200$  in./min.

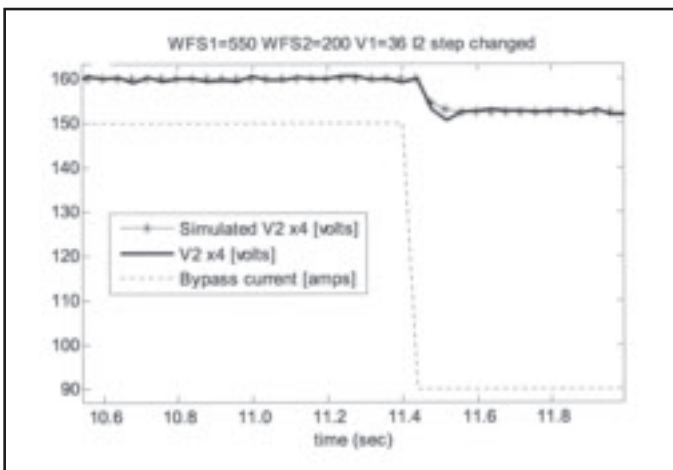


Fig. 13 — Step response when bypass current decreased from 150 to 90 A with  $WFS_2 = 200$  in./min.

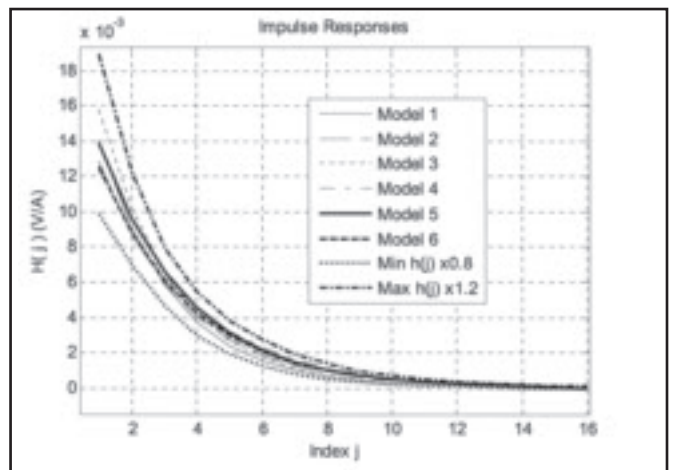


Fig. 14 — Impulse responses and their intervals.

will be made in a relatively small range. Then the base metal current does not change significantly. For most applications, no further control is needed for the

base metal current because small variations should be tolerated. If the base metal current needs to be controlled strictly,  $WFS_2$  can be adjusted together with  $I_2$  and

will not be discussed here. This study focuses on the most fundamental issue: the control of the bypass arc stability. To this end, a control algorithm needs to be de-

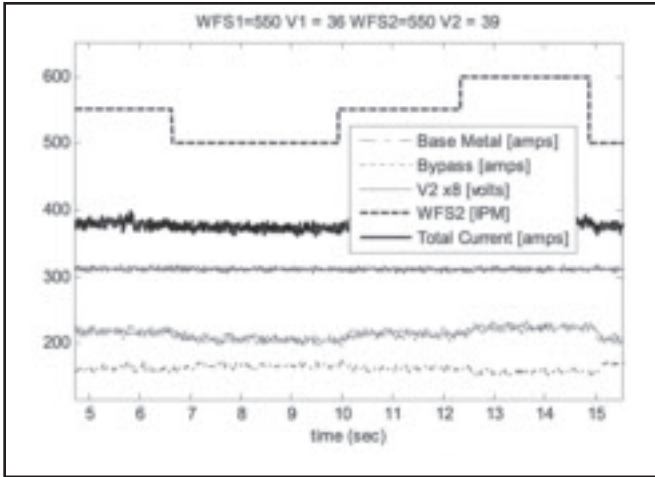


Fig. 15 — Bypass arc stability control. Base metal current is smaller than the bypass current.

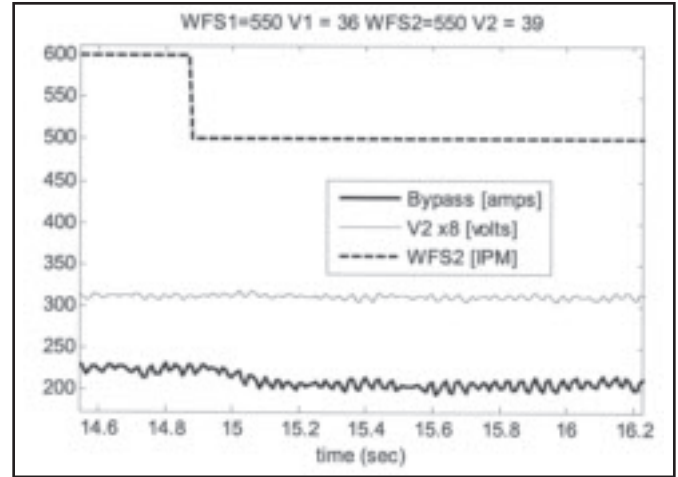


Fig. 16 — Control algorithm response when  $WFS_2$  decreased.

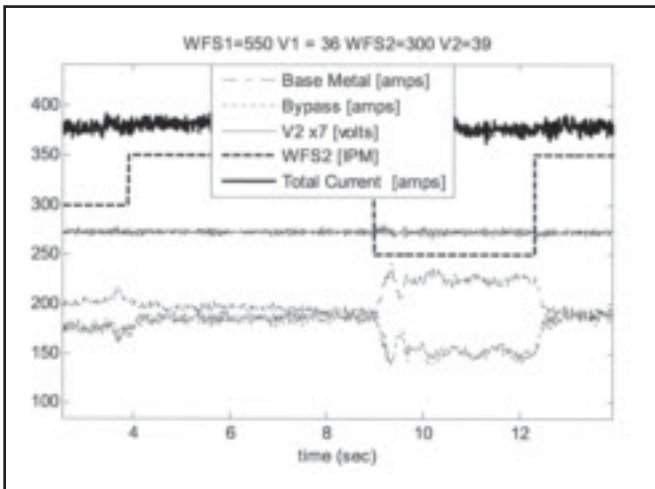


Fig. 17 — Bypass arc stability control. Base metal current is close to the bypass current.

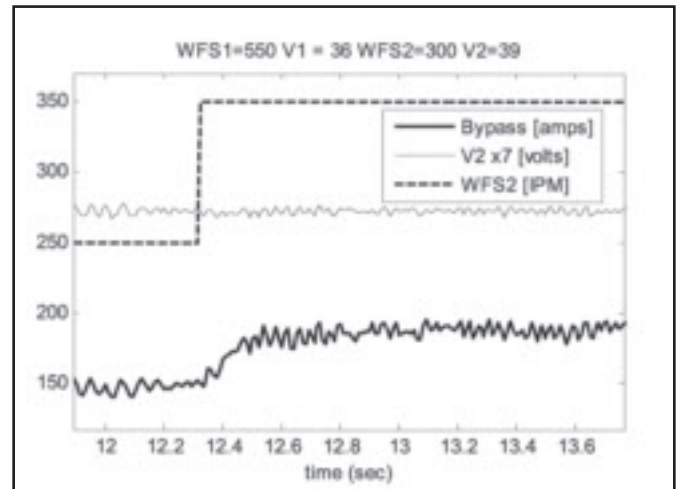


Fig. 18 — Control algorithm response when  $WFS_2$  increased.

signed to adjust the bypass current to maintain the bypass arc voltage  $V_2$  at a desired optimal value while  $WFS_1$ ,  $WFS_2$ , and  $V_1$  are constants. Figure 3 shows the closed-loop control system to be developed. The solid arrow associated with  $WFS_2$  implies that  $WFS_2$  may possibly affect the dynamics of the process, and the dashed arrows associated with  $WFS_1$  and  $V_1$  indicate that the possible effects of  $WFS_1$  and  $V_1$  on the dynamics are insufficient and negligible.

## Control Algorithm

For manufacturing systems, their models are typically affected by the manufacturing conditions. Experiments can be conducted to identify different models with different sets of manufacturing conditions. These models represent the process dynamics in those manufacturing conditions. If all models have the same

structure but different values of parameters, an interval (a minimal value and a maximal value) can be found for each parameter in the model structure. The model can be described using the bounded known intervals for the given ranges of manufacturing conditions. This type of model is referred to as an interval model. The interval model control algorithm is a standard program and does not require any design work. Hence, unlike other techniques such as adaptive control, neural network, and predictive control (Refs. 8–15), the interval model based modeling and control is suitable for welding engineers without systematical training in control. It can be used even if the intervals are relatively small. In particular, the intervals can be artificially enlarged to increase the stability margin of the closed-loop system.

The original interval model control algorithm (Ref. 16) is based on linear sys-

tems described using an impulse response model:

$$y_k = \sum_{j=1}^N h(j)u_{k-j} \quad (1)$$

where  $k$  is the current instant,  $y_k$  is the output at time  $k$ ,  $u_{k-j}$  is the input at  $(k-j)$  ( $j > 0$ ), while  $N$  is the system order and  $h(j)$ 's are the real parameters of the impulse response function. The  $h(j)$ 's ( $1 \leq j \leq N$ ) are unknown but bounded by the intervals:

$$h_{\min}(j) \leq h(j) \leq h_{\max}(j) \quad (j = 1, \dots, N) \quad (2)$$

Where  $h_{\min}(j) \leq h_{\max}(j)$  are the minimum and maximum value of  $h(j)$ 's ( $1 \leq j \leq N$ ) and known. That is, if the parameters of the actual model are bounded by the (nominal) intervals, it is guaranteed  $\lim_{k \rightarrow +\infty} y_k = y^*$ , where  $y^*$  is the set point of the output. The objective of the control algorithm is to de-

termine the feedback control action  $u_k$  such that the closed-loop system achieves the given set point.

Assume the control actions are kept unchanged after instant  $k$ , i.e.,  $\Delta u_{k+j} = 0$  ( $\forall j > 0$ ). Predicting the output  $N$ -step-ahead yields:

$$y_{k+N}(\Delta u_k) = y_k + \sum_{j=2}^N h(j) (u_{k-1} - u_{k-j}) + s(N)\Delta u_k \quad (3)$$

where  $\Delta u_k = u_k - u_{k-1}$ ,  $s(i)$  is the unit step response function and its upper and lower limits  $s_{\max}(i)$  and  $s_{\min}(i)$  satisfy

$$s_{\max}(N)s_{\min}(N) > 0 \quad (4)$$

It is apparent

$$y_{k+N}(\Delta u_k) = y_{k+N}(\Delta u_{k-1}) + s(N)\Delta u_k \quad (5)$$

Where  $y_{k+N}(\Delta u_{k-1}) \stackrel{\Delta}{=} y_{k+N}(\Delta u_k) |_{\Delta u_k=0}$ , i.e., the  $N$ -step-ahead prediction of the output made at instant  $k$  assuming the control actions are not changed at and after instant  $k$ , i.e.,  $\Delta u_{k+j} = 0$  ( $\forall j \geq 0$ ). The control action  $\Delta u_k$  is thus determined:

$$\max y_{k+N}(\Delta u_k) = \max y_{k+N}(\Delta u_{k-1}) + \max(s(N)\Delta u_k) = y^* \quad (6)$$

The control algorithm in Equation 6 can be further written as

$$\max(s(N)\Delta u_k) = y^* - \max y_{k+N}(\Delta u_{k-1}) = y^* - (y_k + \sum_{j=2}^N (\max(a,b))) \quad (7)$$

where  $a = h_{\max}(j)(u_{k-1} - u_{k-j})$ ,  $b = h_{\min}(j)(u_{k-1} - u_{k-j})$ . Denoting  $d_n = \max(s(N)\Delta u_k)$ , the control action can be calculated as

$$\Delta u_k = abs(d_n) \min\left(\frac{sign(d_n)}{s_{\max}(N)}, \frac{sign(d_n)}{s_{\min}(N)}\right) \quad (8)$$

where  $sign(\cdot)$  is a function to return the sign of its parameter. Then, the output of the control algorithm can be calculated as  $u_k = u_{k-1} + \Delta u_k$ .

Figure 4 illustrates the control algorithm described above. In the control system,  $\Delta u_k$  was limited to  $[-10 \text{ A } 10 \text{ A}]$  in each step to avoid an abrupt change in the bypass current. Obviously, an abrupt change in welding current will burn the contact tip. Once the new output  $u_k$  is calculated, the input history  $u$  must be updated.

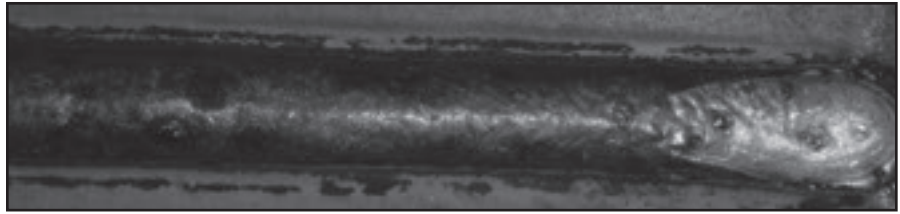


Fig. 19 — Uniform weld bead example.  $WFS_1 = 550 \text{ in./min}$ ,  $V_1 = 36 \text{ V}$ ,  $WFS_2 = 400 \text{ in./min}$ ,  $V_2 = 39 \text{ V}$ ,  $TS = 25 \text{ in./min}$ .

## Process Modeling

To model the consumable DE-GMAW process, step response experiments have been conducted with  $WFS_1$  equal to 14.0 m/min (550 in./min) and  $V_1$  equal to 36 V. Because the bypass wire feed speed may affect the process dynamics, experiments were conducted in major ranges of the bypass wire feed speed: 16.5 m/min (650 in./min) at the high range, 10.2 m/min (400 in./min) in the moderate range, and 5.1 m/min (200 in./min) in the low range. The main welding wire as well as the bypass welding wire was 1.2-mm- (0.045-in.-) diameter low-carbon steel (ER70s-6). Shielding gases (pure argon) were provided through the main gun at a flow of 18.9 L/min (40 ft<sup>3</sup>/h).

Figure 5 illustrates an experiment in the high range of the bypass wire feed speed (650 in./min). It can be seen that step changes in the bypass current resulted in immediate changes in the base metal current as well in the bypass arc voltage. However, the total melting current did not change with the bypass current.

Figure 6 shows the step response when the bypass current increased from 170 to 240 A. A careful examination indicates 1) the process can be approximated by a first order system; 2) the bypass voltage  $V_2$  increased 3.11 V (the signal  $V_2$  was multiplied by a factor 3 such that it can be plotted together with other signals); 3) the time constant is 0.0228 s. Hence, the resultant model can be expressed as a transfer function  $H(s) = 0.0444/(0.0228s + 1)$ , with a static gain equal to 0.0444 V/A. Comparing the simulated  $V_2$  plot to the actual  $V_2$  plot in Fig. 6 suggests that the first-order system has accurately modeled the process.

In another segment of Fig. 6, the bypass current was decreased from 240 to 170 A. This step response can be modeled as another first-order system  $H(s) = 0.0431/(0.0295s + 1)$ , and comparing the simulated  $V_2$  plot to the actual  $V_2$  plot in Fig. 7 suggests that the first-order system has accurately modeled the process.

Figure 8 shows an experiment in the moderate range of the bypass wire feed speed. It can be seen the total current was

maintained around 395 A even though the bypass current changed. Also, the base metal current changed with the bypass current.

Figure 9 gives the segment when the bypass current increased from 130 to 180 A. It can be seen that the system can be modeled as  $H(s) = 0.0395/(0.0228s + 1)$  for the moderate bypass wire feed speed. In the segment shown in Fig. 10, the bypass current decreased from 180 to 130 A. Obviously, the system is still a first-order system with a transfer function  $H(s) = 0.04/(0.0258s + 1)$ .

Another step response experiment in Fig. 11 was performed with a bypass wire feed speed equal to 5.1 m/min (200 in./min). In this experiment, the main wire feed speed was still 14 m/min (550 in./min), and the main arc voltage was 36 V. (The voltages in Figs. 11–13 were multiplied by a factor 4.) It can be seen the total current was not changed when the bypass current changed. However, the bypass voltage did change with the bypass current (at a constant bypass wire feed speed).

In Fig. 12, the bypass current increased from 120 to 150 A. The system can be modeled as  $H(s) = 0.0449/(0.0270s + 1)$ . A step response simulation was done and compared to the experimental data as illustrated in Fig. 13. Similarly, when the bypass current decreased from 150 to 90 A, the system can be modeled as  $H(s) = 0.0414/(0.0277s + 1)$ . The good agreement between the simulated  $V_2$  plot and the actual  $V_2$  plot in Figs. 12 and 13 verifies that the first-order system has accurately modeled the process.

The six transfer functions can be easily converted to impulse responses  $h(j)$ 's by taking the inverse Laplace transform (Ref. 17). These impulse responses are required by the interval model control algorithm and shown in Fig. 14 with a sample period of  $T = 0.01 \text{ s}$ . The minimum and maximum of  $h(j)$ 's were found and formed two curves  $h_{\min}(j) \sim j$  and  $h_{\max}(j) \sim j$ . The two curves can be used to give the intervals for the impulse responses. To improve the stability margin critical applications, the intervals can be artificially enlarged from  $[h_{\min}(j) \ h_{\max}(j)]$  to  $[0.8^* h_{\min}(j) \ 1.2^* h_{\max}(j)]$ . With the enlarged intervals, the truncation of the impulse re-

sponses would cause no effect on the stability of the closed-loop system. Using these intervals, the control algorithm described in Equation 6 and Fig. 4 can be used to calculate the manipulator  $I_2$  based on the feedback of  $V_2$ . In addition, the intervals in Table 1 were obtained with a bypass wire feed speed from 5.1 m/min (200 in./min) to 16.5 m/min (650 in./min). The closed-loop system using these intervals would work when the bypass current varies in a large range.

## Control Experiments

### Experimental Setup

The consumable DE-GMAW setup illustrated in Fig. 1 has been implemented at the University of Kentucky by adding a second GMAW gun and CC power supply to a standard GMAW system. A current sensor was used to feed back the base metal current to the control system. A voltage sensor was utilized to feed back the bypass arc voltage. A second current sensor was used to monitor the bypass current, while an additional voltage sensor was connected to monitor the main arc voltage. The control signals passed D/A boards and isolation boards before they acted on the power supplies. An Olympus high-speed camera equipped with a narrow-banded light filter (central wavelength: 940 nm, bandwidth: 20 nm) was used to record the arc behavior and metal transfer. During experiments, the guns moved together from right to left at a travel speed (TS) of 0.64 m/min (25 in./min). The workpiece was low-carbon steel with a thickness of 0.5 in. (12.7 mm). Pure argon was used as shielding gases only through the main GMAW gun.

### Interval Model Control Experiments

Experiments have been performed to verify the proposed control system for the bypass arc stability. The main wire feed speed was set to 14.0 m/min (550 in./min), but the bypass wire feed speed was changed during experiments. The expected output for the bypass voltage was 39 V while the main arc voltage was 36 V.

In Fig. 15, the bypass wire feed speed was fluctuated around 14 m/min (550 in./min). It can be seen that the bypass voltage was controlled around 39 V even though the bypass wire feed speed changed. An increase in the bypass wire feed speed resulted in an increase in the bypass current due to the closed-loop control. As a result, the feeding-melting balance can be maintained, and a stable bypass arc was obtained. As expected, the total current maintained constant and smooth because of the corresponding change in the base metal current.

A segment of Fig. 15 was zoomed in to

show the response characteristics of the control algorithm — Fig. 16. It can be seen that when the bypass wire feed speed decreased from 15.2 m/min (600 in./min) to 12.7 m/min (500 in./min), the bypass arc voltage was controlled without any obvious change. This verified the appropriate and rapid adjustment in the bypass current from the control algorithm.

A similar experiment was done by decreasing the bypass wire feed speed to a lower level around 7.6 m/min (300 in./min). The experimental results are plotted in Fig. 17. It can be seen that the bypass arc voltage can be controlled at the desired voltage (39 V). Furthermore, the changes in the bypass wire feed speed did not affect the total melting current or the bypass voltage.

When the bypass wire feed speed increased abruptly from 6.4 m/min (250 in./min) to 8.9 m/min (350 in./min), the bypass arc voltage was still controlled at the desired value 39 V shown in Fig. 18. To achieve this, the bypass current was triggered to increase rapidly from 150 to 185 A.

The previously mentioned experiments verified that the proposed control algorithm can effectively control the bypass arc voltage at a desired level resulting in a stable bypass arc. A stable bypass arc in turn allows for a stable consumable DE-GMAW process. Figure 19 demonstrates a uniform weld bead of consumable DE-GMAW.

## Conclusions

This paper details how to control the stability of the bypass arc in the consumable DE-GMAW process. The authors have found:

1. The bypass arc voltage can provide a measurement for the state of the bypass arc to monitor its stability;
2. The interval model provides an effective method to describe the uncertainty of a process whose model depends on manufacturing conditions;
3. The interval model control algorithm only requires the intervals of the model parameters. These intervals may be obtained from a selected set of experiments. Thus, the interval model control algorithm is suitable for manufacturing engineers without systematical training in control;
4. A stable bypass arc plays a critical role in assuring the consumable DE-GMAW process to be an effective manufacturing process; and
5. Closed-loop control experiments verified the effectiveness of the proposed interval model control system.

### Acknowledgment

This research work was funded by the National Science Foundation under grant No. DMI-0355324.

## References

1. Wu, C., Gao, J., and Li, K. H. 1999. Vision-based sensing of weld pool geometry in pulsed TIG welding. *International Journal for the Joining of Materials* 11(1): 18–22.
2. Zhang, Y. M., Zhang, S. B., and Jiang, M. 2002. Keyhole double-sided arc welding process. *Welding Journal* 81(11): 249-s to 255-s.
3. Zhang, Y. M., Zhang, S. B., and Jiang, M. 2002. Sensing and control of double-sided arc welding process. *Journal of Manufacturing Science and Engineering-Transactions of the ASME* 124(3): 695–701.
4. Bicknell, A., Smith, J. S., and Lucas, J. 1994. Arc voltage sensor for monitoring of penetration in TIG welds. *IEEE Proceedings-Science, Measurement and Technology* 141(6): 513–520.
5. Li, L., Brookfield, D. J., and Steen, W. M. 1996. Plasma charge sensor for in-process, non-contact monitoring of the laser welding process. *Measurement Science & Technology* 7(4): 615–626.
6. Lancaster, J. F. 1986. *The Physics of Welding, 2nd Edition*. International Institute of Welding, Pergamon Press, Oxford.
7. Tsai, N. S. 1985. Distribution of the heat and current fluxes in gas tungsten arcs. *Metal. Trans. B* 16B: 841–846.
8. Kawahara, M. 1983. Tracking control system using image sensor for arc welding. *Automatica* 19(4): 357–363.
9. Zhang, Y. M., Kovacevic, R., and Li, L. 1996. Adaptive control of full penetration gas tungsten arc welding. *IEEE Transactions on Control Systems Technology* 4(4): 394–403.
10. Brown, L. J., Meyn, S. P., and Weber, R. A. 1998. Adaptive dead-time compensation with application to a robotic welding system. *IEEE Transactions on Control Systems Technology* 6(3): 335–349.
11. Leith, D. J., and Leithead, W. E. 1999. On microprocessor-based arc voltage control for gas tungsten arc welding using gain scheduling. *IEEE Transactions on Control Systems Technology* 7(6): 718–723.
12. Santos, T. O., Caetano, R. B., Lemos, J. M., and Coito, F. J. 2000. Multipredictive adaptive control of arc welding trailing centerline temperature. *IEEE Transactions on Control Systems Technology* 8(1): 159–169.
13. Li, X. C., Farson, D., and Richardson, R. 2000. Weld penetration control system design and testing. *Journal of Manufacturing Systems* 19(6): 383–392.
14. Zhang, Y. M., and Liu, Y. C. 2003. Modeling and control of quasi-keyhole arc welding process. *Control Engineering Practice* 11(12): 1401–1411.
15. Chen, Q., Sun, Z.-G., Sun, J.-W., and Wang, Y.-W. 2004. Closed-loop control of weld penetration in keyhole plasma arc welding. *Transactions of Nonferrous Metals Society of China (English Edition)* 14(1): 116–120.
16. Zhang, Y. M., and Kovacevic, R. 1997. Robust control of interval plants: A time domain method. *IEEE Proceedings-Control Theory and Applications* 144(4): 347–353.
17. Ziemer, Rodger E., W. H. T., and Fannin, D. Ronald. 1998. *Signals & Systems: Continuous and Discrete*. 4th ed: Prentice Hall.